Preparation and Properties of Cycloolefin Copolymer/Silica Hybrids

Cheng-Fang Ou,[1] Ming-Chieh Hsu[2]

[1]*Department of Chemical and Materials Engineering, National Chin-Yi University of Technology, Taichung County 411, Taiwan, Republic of China*
[2]*Institute of Materials and Chemical Engineering, National Chin-Yi Institute of Technology, Taichung County 411, Taiwan, Republic of China*

Received 3 May 2006; accepted 10 November 2006
DOI 10.1002/app.25983
Published online in Wiley InterScience (www.interscience.wiley.com).

ABSTRACT: Polymer substrates are widely used in the flat-panel-display industry because of their flexibility, light weight, and high power efficiency. However, the lower glass-transition temperatures and thermal stability and higher water/oxygen permeation of cycloolefin copolymers (COCs) constrain their applications in display substrates. In this research, COC/tetraethyloxysilane (TEOS) hybrids were synthesized via a sol–gel process. Differential scanning calorimetry indicated that the glass-transition temperature of the hybrids was higher than that of neat COC and rose significantly as the TEOS content was increased from 1 to 15 wt %. According to an analysis of IR spectra, the fraction of hydrogen-bonded carbonyl groups in the hybrids increased as the TEOS content increased. This meant that the interfacial interaction contributed by hydrogen bonds for the COC/TEOS hybrid system increased as the TEOS content increased from 1 to 15 wt %. On the basis of scanning electron microscopy, the number of dispersed droplets of silica increased as the content of TEOS increased. The decomposition temperatures of the hybrids, investigated with thermogravimetric analysis, were not affected significantly by the addition of TEOS. © 2007 Wiley Periodicals, Inc. J Appl Polym Sci 104: 2542–2548, 2007

Key words: morphology; composites; FTIR

INTRODUCTION

Cycloolefin copolymers (COCs) are amorphous or semicrystalline thermoplastics manufactured by the copolymerization of cycloolefin and olefin monomers. Typically, the cyclic monomer is norbornene or a derivative of norbornene, and the olefin is ethylene or propylene.[1–6] COCs have several useful properties, such as high transparency, low moisture contents and moisture barriers, good mechanical properties, high glass-transition temperatures (T_g's), and high decomposition temperature (T_d's). These novel polymers have potential applications in optical fibers and transparent engineering thermoplastics, as does polycarbonate. Increasing the content of ethylene in COCs increases the flow rate of the polymer melt, and this gives COCs thermoplastic properties that can be processed by extrusion and injection molding.[7–10] The manufacture and properties of COCs have been studied extensively with experimental techniques, with a focus on improvements in the manufacturing technologies.[11–13]

Polymer substrates have widely been used in the flat-panel-display industry because of their flexibility, light weight, and high power efficiency. However, there are some technological difficulties for the realization of a display on a polymer substrate, such as lower thermal stability and higher water/oxygen permeation.[14–18]

The sol–gel process is a convenient method for the preparation of inorganic films or organically modified hybrid materials, in which consecutive reaction steps of hydrolysis and condensation reactions occur between silane groups of the raw materials. The technology has advanced quickly in the past 2 decades. At present, the sol–gel process is not only a manufacturing process for homogeneous inorganic glasses but also a technique for the synthesis of organic–inorganic hybrid materials for various applications in optical and nonlinear devices, electrical and organically modified ceramic materials, reinforced elastomers and plastics, and biochemistry.[19–24] In these applications, important properties such as the appearance, transparency, and phase behavior depend on the development of an inorganic silicate structure and the interfacial interactions between the organic and inorganic phases in the hybrid materials. The silica molecules act as reinforcing agents, making

Correspondence to: C.-F. Ou (oucf@ncit.edu.tw).
Contract grant sponsor: National Science Council of the Republic of China; contract grant number: NSC94-2216-E-167-002.

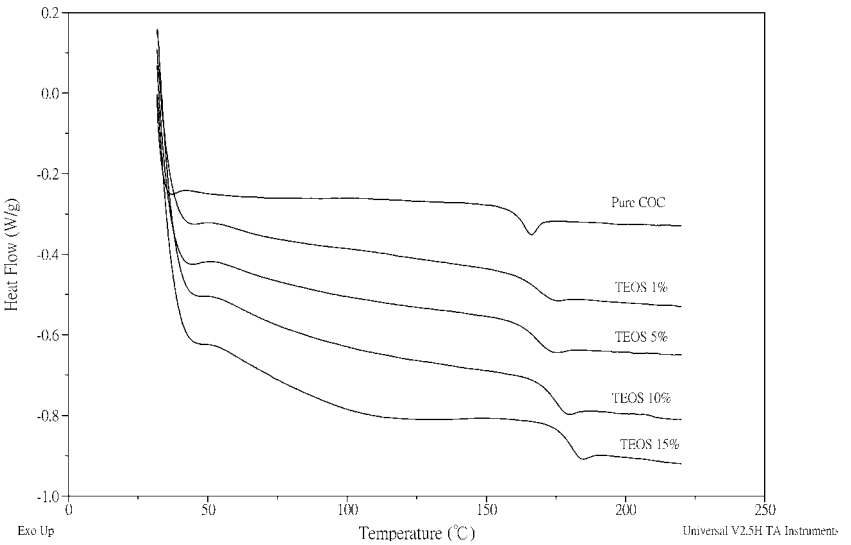

Figure 1 DSC thermogram curves of pure COC and COC/TEOS hybrids.

the polymers harder, giving them better mechanical properties, improving their thermal stability, and lowering their water/oxygen permeation and coefficient of thermal expansion. Hence, studies on these topics are very important for the advancement of this technology. Many studies have been devoted to the preparation of polymer/silica hybrid materials with organic monomers and inorganic precursors such as tetraethyloxysilane (TEOS) through *in situ*, acid-catalyzed sol–gel processes.[25–28] In these hybrids, the inorganic molecules and organic molecules interconnect by chemical covalent bonds, hydrogen bonds, or physical interactions. The structure of a hybrid depends on the processing conditions, such as the type of catalyst, the pH value, the water quantity, the solvent system, and the reaction temperature. Some acrylic polymer/silica hybrids show a yellowing phenomenon caused by the remaining initiators or nonpolymeric monomers in the final products.

In this study, COC/silica hybrids were constructed from COCs and inorganic TEOS synthesized via an acid-catalyzed sol–gel process. The structure, morphology, thermal resistance, and light transmittance of the hybrids were evaluated and studied with differential scanning calorimetry (DSC), thermogravimetric analysis (TGA), Fourier transform infrared (FTIR), scanning electron microscopy (SEM), and ultraviolet–visible (UV–vis) spectrometry.

EXPERIMENTAL

Materials

The COC copolymer was a commercial product (Arton) manufactured by Japan Synthetic Rubber Co., Ltd. The chemical structure of COC is as follows:

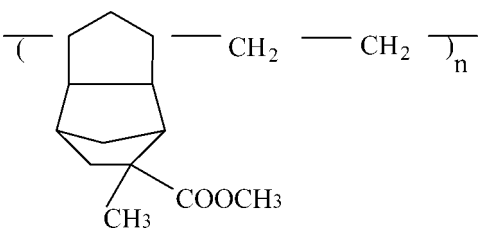

TEOS (i.e., tetraethyl orthosilicate; Acros) and tetrahydrofuran (Fisher), which was used as a solvent, were used as received. Hydrochloric acid (Union Chemical Works) was applied as a catalyst, and deionized water was generated with a Milli-Q plus water purification system (Millipore).

Preparation of the desired hybrid films

The COC was dissolved in tetrahydrofuran first. A TEOS solution was then prepared with an H^+/H_2O/ethanol/TEOS molar ratio of 0.025/25/5/1. Various organic–inorganic ratios (99/1, 95/5, 90/10, and 85/15 w/w) for the COC/TEOS mixture were stirred for 1 h at room temperature, poured into a sealed reactor, and allowed to react at 55°C for 6 h. After the

TABLE I
T_g Values of the COC/TEOS Hybrids

Composition	T_g (°C)
Pure COC	161.9
1 wt % TEOS	167.1
5 wt % TEOS	167.2
10 wt % TEOS	173.7
15 wt % TEOS	179.5

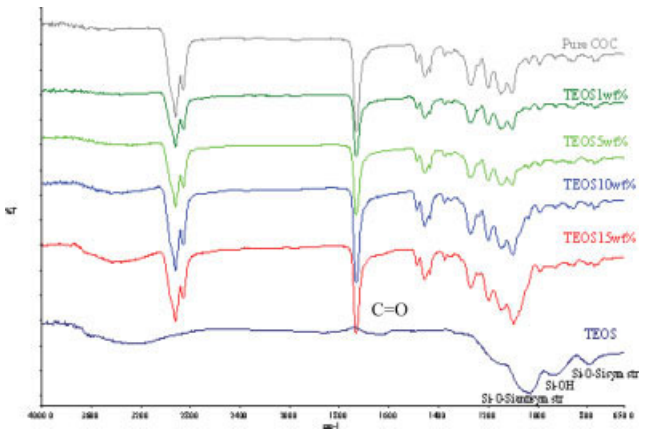

Figure 2 FTIR spectra of pure COC and COC/TEOS hybrids. [Color figure can be viewed in the online issue, which is available at www.interscience.wiley.com.]

sol–gel reaction, the mixture was removed from the reactor, poured into an aluminum mold, and then dried at 70°C *in vacuo* for 24 h. The postreaction was conducted at 105°C *in vacuo* for 24 h to remove the residual solvent and byproducts (water and alcohol). For comparison, neat COC was also made with the same procedure.

Characterization

DSC measurements were performed with a TA 2010 analyzer (TA Instruments, New Castle, DE). The sample was dried at 60°C for 6 h in a vacuum oven before DSC characterization. Appropriate amounts of the samples (ca. 5 mg) were sealed in aluminum sample pans. DSC analyses of these hybrid materials were then conducted under a dry nitrogen atmosphere. The samples were heated first to 250°C and kept for 3 min in the hermetic cell to remove the thermal history. The samples were then cooled to 30°C at a rate of 20°C/min, and then a second heating was performed at a rate of 20°C/min to 250°C. The T_g results from the second heating thermograms were the averages of three samples.

TGA of the dried hybrids was performed with a TGA 910 (TA Instruments, New Castle, DE) under a nitrogen atmosphere at a heating rate of 20°C/min. The structural characteristics of the raw materials and hybrids were analyzed with a Nicolet Avatar 320 FTIR spectrophotometer in the special range of 4000–400 cm^{-1} with a 4-cm^{-1} resolution. The morphology of the hybrid material was obtained from SEM observations with a JEOL JSM-6360. The optical transmittance analysis was measured with a Varian Cary-100 UV–vis spectrometer with wavelengths ranging from 300 to 800 nm.

RESULTS AND DISCUSSION

T_g of the hybrids

DSC was introduced to investigate T_g of these hybrids. Figure 1 shows the DSC thermogram curves of neat COC and hybrid materials. There is a distinct single T_g located in the region from 160 to 185°C in all the hybrids, and the T_g values are listed in Table I. T_g of pure COC was 161.9°C. The T_g values of the hybrids were higher than that of neat COC. The T_g values of these hybrids rose with the increasing content of inorganic silica (TEOS) in the hybrids. T_g increased to 167.1°C for the 1 wt % TEOS hybrid. The extremely high value of T_g was 179.5°C, 17.6°C higher than that of neat COC, when the TEOS concentration increased to 15 wt %. These data confirm the miscibility of TEOS and COC when the TEOS concentration of the hybrid was 1–15 wt %. The increasing crosslinking density of the hybrids with TEOS concentrations from 1 to 15 wt %, due to the developed inorganic silicate structure, brought about a reduction of the molecular mobility and the elevation of T_g.[29–31]

FTIR characterization

The IR spectra of the raw materials and hybrids are shown in Figure 2. In this figure, the absorption peaks of the silica structure (Si—OH stretching at 939 cm^{-1} and Si—O—Si asymmetric stretching and symmetric stretching at 1083 and 791 cm^{-1}, respectively) are all well resolved. In the COC/TEOS hybrids, the tether between the silica and COC chains caused the band absorptions to correspond to the C—O—C groups in the COC chains, and the Si—O—Si groups in the silica significantly over-

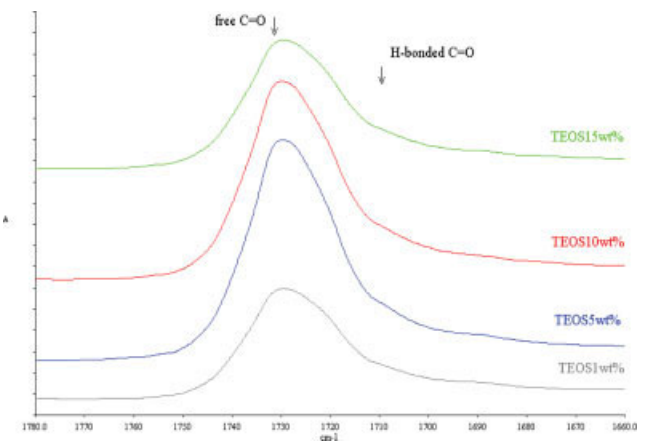

Figure 3 Scale-expanded IR spectra in the carbonyl stretching region of COC/TEOS hybrids. [Color figure can be viewed in the online issue, which is available at www.interscience.wiley.com.]

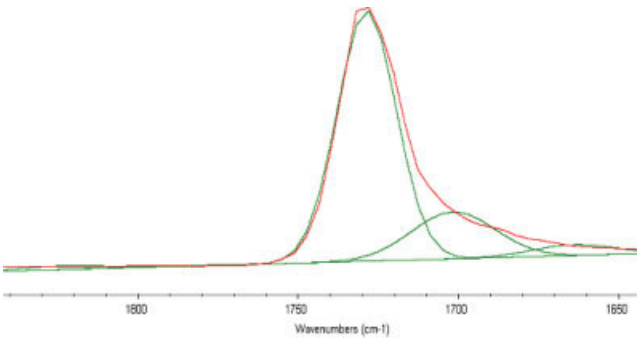

Figure 4 Curve fitting for the carbonyl absorption of the 5 wt % TEOS hybrid. [Color figure can be viewed in the online issue, which is available at www.interscience.wiley.com.]

lapped and, as shown in the band range of 1300–1000 cm^{-1} in the IR spectrum of the hybrid, could not be clearly distinguished. In addition, all the synthesized hybrids had IR absorption at about 1728 cm^{-1}, which corresponded to the carbonyl group C=O stretching vibration on the side chain of COC. These absorption peaks of the carbonyl group for the hybrids were obtained with an FTIR spectrophotometer and are sketched in Figure 3 in the spectral range of 1825–1525 cm^{-1}. In this figure, there is an obvious shoulder at about 1728 cm^{-1} with increasing content of the TEOS component. This absorption was constructed by two distinct peaks at about 1728 and 1710 cm^{-1}, which belonged to the free and hydrogen-bonded carbonyl groups, respectively. With curve-fitting analysis, the absorption band of the carbonyl groups could be readily separated into two peaks by Gaussian curve fitting.[32,33] The fraction of hydrogen-bonded carbonyl could be calculated with the following equation suggested by Coleman and coworkers:[33–35]

$$f_{\text{bonded}} = A_{\text{bonded}}/(A_{\text{bonded}} + A_{\text{free}}) \quad (1)$$

where A_{bonded} is the area of the hydrogen-bonded carbonyl absorption, A_{free} is the area of the free carbonyl absorption, and f_{bonded} is the fraction of the hydrogen-bonded carbonyl groups. In addition, the ratio of the absorptive coefficients of the two bands for the hydrogen-bonded and free carbonyl is presumed to be equivalent in this study.[36]

With this method, the carbonyl stretching absorption of the hybrids could be easily separated into two Gaussian peaks at about 1728 and 1710 cm^{-1}, which were the absorptions of the free carbonyl and hydrogen-bonded carbonyl groups, as shown in Figure 4 for the 5 wt % TEOS hybrid. These values of the fraction of the hydrogen-bonded carbonyl groups for the hybrid materials were calculated and are shown in Table II. From the hydrogen-bonding analysis, the fraction of hydrogen-bonded carbonyl groups for the 1 wt % TEOS hybrid was 14.3%. Although the TEOS concentration increased to 15 wt %, the concentration of the hydrogen-bonded carbonyl groups for the COC/TEOS hybrid was increased continuously to the extremely high value of 26.4%. This means that the interfacial interaction contributed from the hydrogen bonds for the COC/TEOS hybrid system increased as the TEOS content increased from 1 to 15 wt %.

Morphology investigation

A transparent and smooth specimen was obtained for neat COC after the synthesis. In addition, the specimens were transparent, except for the 15 wt % TEOS hybrid. The 15 wt % TEOS specimen was translucent. It was concluded that the organic and inorganic phases were compatible in the COC/TEOS hybrids with TEOS concentrations lower than 10 wt %.

Figure 5 shows SEM micrographs of the fracture surfaces of the samples. The fractured surface of pure COC was very smooth and homogeneous [Fig. 5(a)]. The morphology of the fractured surfaces of the COC/TEOS hybrid with 5 wt % TEOS was the same as that of pure COC [Fig. 5(b)]. This result indicates that the miscibility of COC and silica was good for the hybrids with TEOS concentrations lower than 5 wt %. In Figure 5(c,d), the morphology of the COC/TEOS hybrids with 10 and 15 wt % TEOS show an obvious change from that of pure COC. The dispersed droplet dispersions of silica were embedded in the COC matrix and were set loose

TABLE II
Curve-Fitting Results from the IR Spectra of the COC/TEOS Hybrids

	Free C=O		Hydrogen-bonded C=O		
Hybrid material	ν (cm^{-1})	A_{free} (%)	ν (cm^{-1})	A_{bonded} (%)	f_{bonded} (%)
Pure COC	1729.0	100	—	0.0	0.0
1 wt % TEOS	1728.3	85.7	1704.3	14.3	14.3
5 wt % TEOS	1728.6	81.7	1708.8	18.3	18.3
10 wt % TEOS	1729.9	74.8	1713.6	25.2	25.2
15 wt % TEOS	1728.8	73.6	1710.7	26.4	26.4

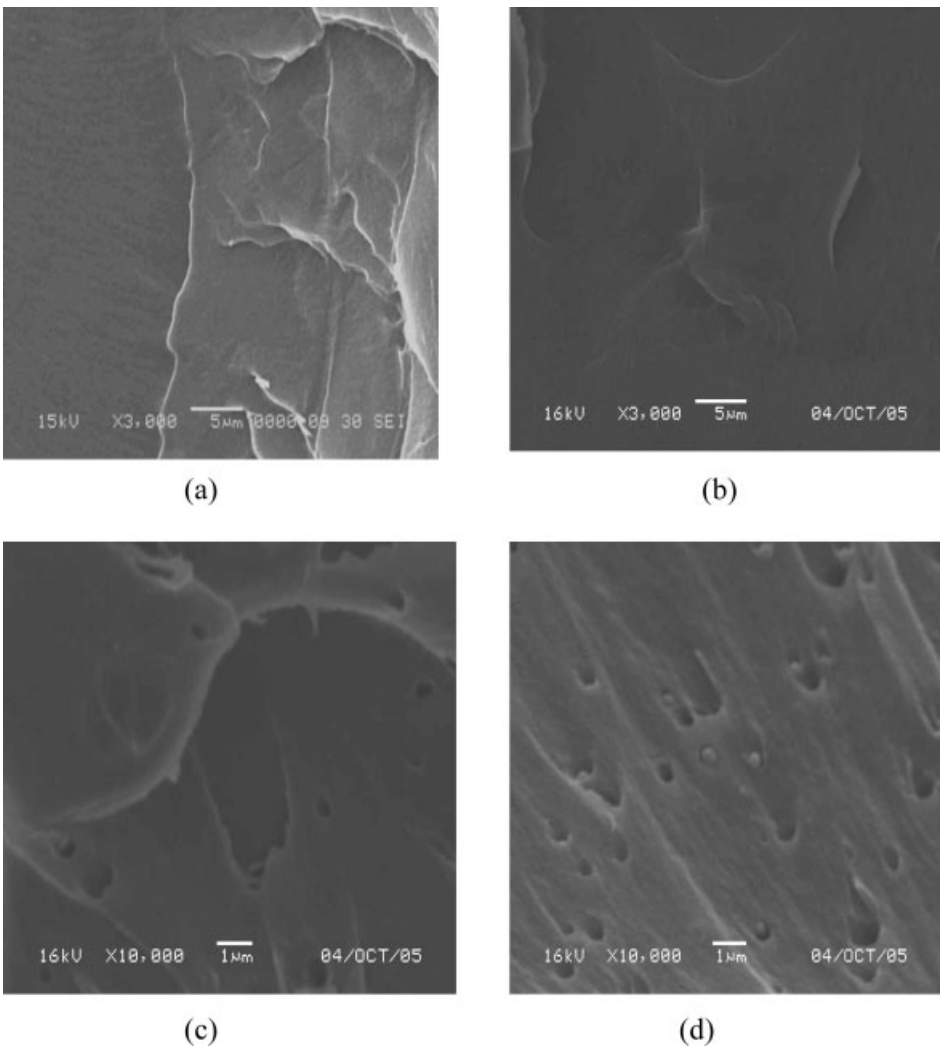

Figure 5 SEM micrographs of the fracture surfaces of COC/TEOS hybrids: (a) pure COC, (b) 5 wt % TEOS, (c) 10 wt % TEOS, and (d) 15 wt % TEOS.

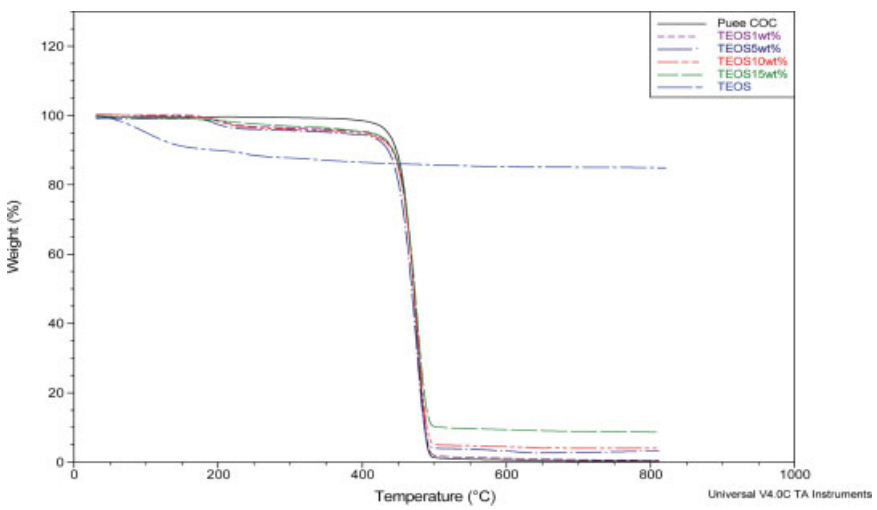

Figure 6 TGA curves of COC/TEOS hybrids. [Color figure can be viewed in the online issue, which is available at www.interscience.wiley.com.]

from the matrix during the fracture. The shapes of the dispersed droplets were spherical or elliptical geometries, with the domain sizes ranging from 0.2 to 0.5 μm. The number of dispersed droplets in the 15 wt % TEOS hybrid was more than that in the 10 wt % TEOS hybrid. This reveals that the number of dispersed droplets increased with increasing TEOS content.

Thermal stability of the hybrids

The thermal decomposition behaviors of the hybrids were investigated by TGA at a heating rate of 20°C/min under a nitrogen atmosphere, as illustrated in Figure 6. The data for the degradation temperatures were collected from derivative thermogravimetry (DTG; not shown) curves and are listed in Table III. We found that the COC decomposed in a single stage (main degradation stage) and that its T_d was 475.0°C. There was about 16.4 wt % weight loss for neat TEOS at a temperature greater than 100°C. In the COC/TEOS hybrids, there were two stages of weight loss. The first stage of degradation (predegradation stage) occurred at 180–230°C before the main degradation, as shown in Figure 6. The main degradation stage started at 450°C. A review presented by Zhou et al.[37] illustrated that the occurrence of predegradation resulted from the elimination of methanol and water produced from the further hydrolysis and polycondensation processes between Si—OH and Si—OCH_3 groups or themselves. In this study, the predegradation resulted from the elimination of methanol and water produced from the further hydrolysis and polycondensation processes between Si—OH and Si—OC_2H_5 groups or themselves.

The hybrids possessed the same T_d (main degradation stage) as that of COC. Table III also shows that the quantity of the residue at 650°C increased with an increasing amount of TEOS. Because the silica content in the hybrids was proportional to the residual weight content at 650°C in the TGA trace, the silica content increased with an increasing amount of TEOS in the hybrids.

TABLE III
TGA Data for the COC/TEOS Hybrids

Composition	T_d (°C)[a]	Residue at 650°C (wt %)
Pure COC	475.0	0.0
TEOS 1 wt %	476.3	0.4
5 wt % TEOS	474.8	3.7
10 wt % TEOS	474.9	3.8
15 wt % TEOS	475.4	8.9
Pure TEOS	—	83.6

[a] Obtained from the peaks of the DTG data.

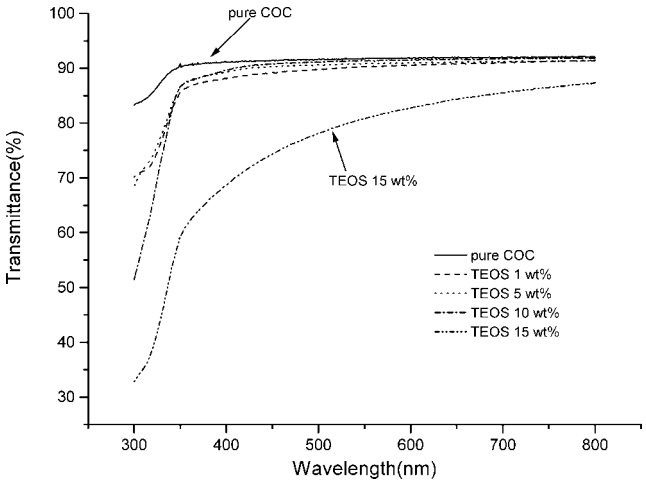

Figure 7 Transmittance spectra of pure COC and COC/TEOS hybrids.

Transmittance of the hybrids

Figure 7 shows the light transmittance of pure COC and COC/TEOS hybrids. The thickness of these films was about 100 μm. The transmittance of pure COC at 550 nm was as high as 91.7%. The spectra show that the visible region (400–700 nm) was not affected by the presence of less than 10 wt % TEOS and retained the high transparency of the COC. The transmittance of the hybrid with 15 wt % TEOS decreased to 80.8% at 550 nm. According to the SEM micrograph of the 15 wt % TEOS hybrid [Fig. 5(d)], the large size (0.2–0.5 μm) and higher content of silica dispersed in the COC matrix resulted in lower light transmittance. The finer size of the silica, accompanied by good compatibility between silica and COC, might be the reason for the high light transmittance of the COC/TEOS hybrids with less than 10 wt % TEOS. The transmittance of the COC/TEOS hybrids was still higher than that (ca. 90%) required for optical and other applications, except for the hybrid with 15 wt % TEOS.

CONCLUSIONS

In this study, COC/TEOS hybrids exhibited higher T_g values than pure COC, and T_g rose as the TEOS content increased. The fraction of hydrogen-bonded carbonyl groups in the COC for the COC/TEOS hybrids increased as the TEOS content increased. This meant that the interfacial interaction contributed by hydrogen bonds for the COC/TEOS hybrid system increased as the TEOS content increased from 1 to 15 wt %. The COC/TEOS hybrids exhibited the same thermal resistance as the pure COC polymer. The light transmittance of the COC/TEOS hybrids was still higher than 90% with TEOS concentrations up to 10 wt % and satisfied the need of optical and other applications.

References

1. Marathe, S.; Mohandas, Y. P.; Sivaram, S. Macromolecules 1995, 28, 7318.
2. Marathe, S.; Sivaram, S. Macromolecules 1994, 27, 1083.
3. Harrington, B. A.; Crowther, D. J. J Mol Catal A 1998, 128, 79.
4. Kaminsky, W. Papra Rev Rep 1999, 10, 28.
5. Yeh, J. M.; Weng, C. J.; Huang, K. Y.; Huang, H. Y.; Yu, Y. H. J Appl Polym Sci 2004, 94, 400.
6. Huang, W. J.; Chang, F. C. J Polym Res 2003, 10, 195.
7. Kaminsky, W.; Bark, A.; Arndt, M. Macromol Chem Macromol Symp 1991, 47, 83.
8. Kaminsky, W.; Bark, A. Polym Int 1992, 28, 251.
9. Herfert, N.; Montag, P.; Fink, G. Macromol Chem 1993, 194, 3167.
10. Kaminsky, W. Macromol Chem Phys 1996, 197, 3907.
11. Alt, F. P.; Heitz, W. Acta Polym 1998, 49, 477.
12. Ruchatz, D.; Fink, G. Macromolecules 1998, 31, 4681.
13. Kaminsky, W. Catal Today 1994, 20, 257.
14. Burrows, P. E.; Graff, G. L.; Gross, M. E.; Martin, P. M.; Shi, M. K.; Hall, M.; Mast, E.; Bonham, C.; Bennett, W.; Sullivan, M. B. Display 2001, 22, 65.
15. Kloppel, M.; Kriegeis, W.; Meyer, B. K.; Scharmann, A.; Daube, C.; Stollenberg, J.; Tube, J. Thin Solid Films 2000, 365, 139.
16. Fahland, M.; Karlsson, P.; Charton, C. Thin Solid Films 2001, 392, 334.
17. Lee, M. J.; Judge, C. P.; Wright, S. W. Solid-State Electron 2000, 44, 1431.
18. Henry, B. M.; Erlat, A. G.; McGuigan, A.; Grovenor, C. R. M.; Briggs, G. A. D.; Tsukahara, Y.; Miyamoto, T.; Niijima, T. Thin Solid Films 2001, 382, 194.
19. Brinker, C. J.; Scherer, G. W. Sol–Gel Science: The Physics and Chemistry of Sol–Gel Processing; Academic: London, 1990.
20. Hoh, K. P.; Ishida, H.; Koenig, J. L. Polym Compos 1990, 11, 121.
21. Bahulekar, R. V.; Prabhune, A. A.; Sivaraman, H.; Ponrathnam, S. Polymer 1993, 34, 163.
22. Novak, B. M. Adv Mater 1993, 5, 422.
23. Zarzycki, J. J Sol–Gel Sci Technol 1997, 8, 17.
24. Calvert, P. Nature 1991, 353, 501.
25. Weetall, H. H.; Robertson, B.; Cullin, D.; Brown, J.; Walch, M. Biochim Biophys Acta 1993, 1142, 211.
26. Reetz, M. T.; Zonta, A.; Simpelkamp, J. Biotechnol Bioeng 1996, 49, 527.
27. Park, S. H.; Lee, S. B.; Ryu, D. D. Y. Biotechnol Bioeng 1981, 23, 2591.
28. Ruckenstein, E.; Wang, X. Biotechnol Bioeng 1992, 39, 679.
29. Norisuye, T.; Shibayama, M.; Tamaki, R.; Chujo, Y. Macromolecules 1999, 32, 1528.
30. Chan, C. K.; Chu, I. M.; Lee, W.; Chin, W. K. Macromol Chem Phys 2001, 202, 911.
31. Chan, C. K.; Chu, I. M.; Ou, C. F.; Lin, Y. W. Mater Lett 2004, 58, 2243.
32. Kioul, A.; Mascia, L. J. Non-Cryst Solids 1994, 175, 169.
33. Wu, H. D.; Ma, C. C. M.; Chu, P. P. Polymer 1997, 38, 5419.
34. Coleman, M. M.; Graf, J. F.; Painter, P. C. Specific Interactions and the Miscibility of Polymer Blends; Technomic: Lancaster, PA, 1991.
35. Coleman, M. M.; Yang, X.; Painter, P. C. Macromolecules 1992, 25, 4414.
36. Wang, F. Y.; Ma, C. C. M.; Hung, A. Y. C.; Wu, H. D. Macromol Chem Phys 2001, 202, 2328
37. Zhou, W.; Dong, J. H.; Qiu, K. Y.; Wei, Y. J Polym Sci Part A: Polym Chem 1998, 36, 1607.